Direct Electron Transfer Kinetics in Horseradish Peroxidase Electrocatalysis

Rafael Andreu,*,† Elena E. Ferapontova,‡ Lo Gorton,§ and Juan Jose Calvente*,†

Departamento de Química Física, Universidad de Sevilla, 41012-Sevilla, Spain, School of Chemistry, University of Edinburgh, Edinburgh EH9 3JJ, United Kingdom, and Department of Analytical Chemistry, Lund University, SE-221 00 Lund, Sweden

Received: July 7, 2006; In Final Form: October 23, 2006

The study of direct electron transfer between enzymes and electrodes is frequently hampered by the small fraction of adsorbed proteins that remains electrochemically active. Here, we outline a strategy to overcome this limitation, which is based on a hierarchical analysis of steady-state electrocatalytic currents and the adoption of the "binary activity" hypothesis. The procedure is illustrated by studying the electrocatalytic response of horseradish peroxidase (HRP) adsorbed on graphite electrodes as a function of substrate (hydrogen peroxide) concentration, electrode potential, and solution pH. Individual contributions of the rates of substrate/enzyme reaction and of the electrode/enzyme electron exchange to the observed catalytic currents were disentangled by taking advantage of their distinct dependence on substrate concentration and electrode potential. In the absence of nonturnover currents, adoption of the "binary activity" hypothesis provided values of the standard electron-transfer rate constant for reduction of HRP Compound II that are similar to those reported previously for reduction of cytochrome *c* peroxidase Compound II. The variation of the catalytic currents with applied potential was analyzed in terms of the non-adiabatic Marcus-DOS electron transfer theory. The availability of a broad potential window, where catalytic currents could be recorded, facilitates an accurate determination of both the reorganization energy and the maximum electron-transfer rate for HRP Compound II reduction. The variation of these two kinetic parameters with solution pH provides some indication of the nature and location of the acid/base groups that control the electronic exchange between enzyme and electrode.

Introduction

Enzymatic redox centers are embedded into a protein matrix, which plays a key role in catalysis, and it also helps to isolate the redox center from adventitious reactants. The low electronic conductivity of the surrounding amino acid chains makes electron-transfer rates prohibitively slow in most orientations around the redox center. In spite of these difficulties, direct (mediatorless) electron transfer (DET) between several electrode surfaces and more than 40 redox enzymes has been observed already,[1] paving the way for the development of "third generation" biosensors.[2] Beyond its elegant simplicity, analysis of the current generated in DET experiments can be exploited, under either nonturnover or catalytic conditions, to gain further insight into the mechanisms of electron transfer in biological systems.[3]

Horseradish peroxidase (HRP) is a glycosylated plant peroxidase (MW $\approx$ 44 kDa) that catalyzes the reduction of hydrogen peroxide by a variety of organic and inorganic cosubstrates.[4] It contains one ferriprotoporphyrin IX as the heme prosthetic group. HRP has found widespread use as a component of clinical diagnostic kits and biosensors.[5] The basic catalytic scheme involves three steps: (i) oxidation of the native ferric enzyme by hydrogen peroxide to form an oxyferryl Fe^{IV}=O group and a porphyrin π cation radical, denoted as the Compound I intermediate, (ii) reduction of the cation radical of Compound I by a one-electron donor to give Compound II, and (iii) reduction of the oxyferryl group by a second one-electron donor molecule to revert the enzyme back to its resting ferric state. The last two reduction steps are accompanied by the uptake of two protons and the removal of a water molecule. Detailed molecular structures of these catalytic intermediates have become available recently from X-ray diffraction measurements.[6]

Direct electron transfer of HRP adsorbed on a carbon electrode was first reported by Yaropolov et al.[7] in 1978 and, since then, it has also been observed on a variety of electrode materials.[8] However, most of these studies involve an interconversion between the Fe(III) and Fe(II) oxidation states of the enzyme, as can be easily inferred from the location of the DET current at rather negative potential values (typically ≤ -0.1 V vs AgCl|Ag at pH = 7).[8,9] Alternatively, formal potentials of the HRP Compound I/Compound II and Compound II/Fe(III) redox couples take rather positive values (close to 0.7 V vs AgCl|Ag at pH = 7),[10,11] thus allowing for a highly efficient H_2O_2 reduction mechanism operating at small overvoltages. Nonturnover currents associated with HRP Compound I and Compound II have not been reported thus far, and evidence for DET comes from the observation, in the presence of adsorbed HRP, of H_2O_2 reduction currents at positive potential values that are consistent with the involvement of Compound I and Compound II as catalytic intermediates. The lack of detectable nonturnover signals is also found with other electrocatalytic enzymes, as in the case of laccases adsorbed on carbon,[12] and it is likely to be caused by the small fraction of adsorbed enzymes that meet the two basic requirements to act as a DET bioelectrocatalyst: (a) an adequate orientation that facilitates

* Corresponding authors: Phone: +34-954557177. Fax: +34-954557174. E-mail: fondacab@us.es; pacheco@us.es.
† Universidad de Sevilla.
‡ University of Edinburgh.
§ Lund University.

10.1021/jp064277i CCC: $37.00
Published on Web 12/19/2006

the electron exchange between the electrode and the enzyme prosthetic group,[13] and (b) an appropriate conformational structure of the amino acid residues that helps to form and stabilize the catalytic intermediates.[14]

In this report we present a detailed steady-state analysis of the nonmediated bioelectrocatalytic activity of adsorbed HRP, as a function of substrate concentration, electrode potential, and solution pH. Under steady-state conditions, catalytic currents can be modeled as a series connection of enzyme/substrate and enzyme/electrode kinetic events.[15,16] We show how these two contributions can be decoupled by taking advantage of their distinct dependence on substrate concentration and electrode potential. The absence of nonturnover currents precludes the experimental determination of the surface concentration of active enzymes and the assignment of absolute values to the rate constants. Instead of presenting our results in terms of relative variations of the rate parameters, we have adopted the "binary activity" hypothesis[15,17] (i.e., adsorbed enzymes are considered to be either fully active or fully inactive) that allowed us to estimate the amount of active enzymes and to discuss the observed electrocatalytic behavior on a more clear basis. By embracing this hypothesis, the enzyme/substrate kinetics are assumed to be identical to those derived from studies in homogeneous solution,[4,18] and acquisition of new kinetic information becomes restricted to the last two charge-transfer steps of the HRP catalytic cycle.

Electrochemical techniques provide a convenient way to vary the thermodynamic driving force for electron-transfer reactions. According to Marcus theory,[19] the reorganization energy for electron transfer can be determined by correlating changes in reaction rate with those in the reaction driving force or, in electrochemical terms, by analyzing the dependence of the recorded current on the applied potential. Besides, the protein matrix provides a weak electronic coupling between the electrode and the enzyme prosthetic group[20] so that protein DET is usually assumed to take place within the non-adiabatic electron-transfer regime.[21] Here, we will show how the analysis of the steady-state catalytic current over a large overvoltage range facilitates an accurate determination of both the reorganization energy and the extent of electronic coupling.

The activities of many enzymes vary with pH because of the presence of ionizable acid/base groups in the active sites. The pK_a values of these catalytically relevant groups are expected to depend on the oxidation state of the enzyme and, in the case of HRP, they will differ for Compound I, Compound II, and the native ferric form.[22] However, the fact that the rate of formation of Compound I is largely independent of pH,[4] that the rate of reduction of Compound I is much faster than that of Compound II,[23,24] and the availability of the pH dependence of the Compound I/Compound II and Compound II/ferric form redox potentials[10,11] helps to simplify the analysis of the pH influence on the catalytic currents. In a previous study on the effect of pH on the electrocatalytic efficiency of adsorbed HRP,[8,25] first-order kinetics with respect to proton concentration were reported within the $6 < pH < 8$ interval. Here, we have extended the pH interval down to pH 4 and have found that the catalytic current displays a bell-shaped dependence on solution pH. This behavior is similar to that observed in the oxidation of several phenols by HRP compound II in solution,[26,27] though the two rate-controlling pK_a values are not the same. Though the identification of the residues responsible for these protonation processes is beyond the scope of this work, the dependence of the reorganization energy and of the electronic coupling on the solution pH will be shown to give some hints and to set some restrictions on their identification.

Experimental Section

HRP (isoenzyme C) from Sigma, St. Louis, MO [1100 U mg^{-1} (ABTS)], and other reagents from Merck, Darmstadt, Germany, were used. All chemicals were of analytical grade and used as received. All solutions were prepared with deionized Milli-Q water (Millipore, Bedford, MA).

Steady-state voltammetry was carried out in a standard three-electrode electrochemical cell. The working electrode was the disk surface of a solid spectroscopic graphite rod (3.05 mm in diameter, SGL Carbon AG, Werk Ringsdorff, Bonn, Germany, type RW001, fitted in Teflon holders). An $Ag|AgCl|KCl_{sat}$ electrode and a Pt foil served as reference and auxiliary electrodes, respectively. All potential values have been shifted 0.197 V so that they are referred to the normal hydrogen electrode (NHE). Steady-state voltammetry was performed with a rotating disk electrode (RDE) system (Tacussel Electronique, Villeurbanne, France) at a rotation rate of 959 rpm, to minimize concentration polarization. Within the potential range of interest, stationary currents were recorded every 50 mV, after waiting for 45 s at each potential in order to reach the steady-state regime. The electrodes were connected to a three-electrode potentiostat AUTOLAB PGSTAT 30 (Eco Chemie B. V., Utrecht, Netherlands) equipped with a GPES 4.9 software (Eco Chemie). The electrolyte was 0.01 M phosphate buffer, containing 0.15 M NaCl, (PBS) in the pH range from 4.0 to 8.0. Solutions were deoxygenated by bubbling argon, and all measurements were made at room temperature (22 ± 1 °C).

The surface of the graphite disk electrodes was cut, polished on fine emery paper (Tufbak Durite, P2000), and rinsed carefully with water. The electrochemically active surface area of the electrodes was 0.20 ± 0.03 cm^2 as estimated from the Cottrell slopes of chronoamperometric currents recorded in 1 mM ferricyanide solutions. For the adsorption of HRP, the electrodes were immersed in a 1 mg mL^{-1} HRP solution in PBS, pH 6.0, for 2 h at room temperature. Longer incubation times, including overnight exposure to a 1 mg mL^{-1} HRP solution at 4 °C, produced similar results so that adsorption saturation is apparently reached under these deposition conditions. Then, the electrodes were rinsed in PBS, inserted into the cell, and used in the following measurements. Before the measurements, the solutions were de-oxygenated with argon for at least 30 min. The reproducibility of the data was verified by measurements with at least three equivalently prepared electrodes. For a given set of 10 freshly prepared electrodes, catalytic currents were found to be reproducible within 20%. The stability of the response within the 0.1 V/0.6 V potential range was checked in the presence of 0.1 mM hydrogen peroxide; a current decay $\leq 10\%$ was observed during 60 min of continuous recording of the steady-state currents.

Results and Discussion

A. Kinetic Modeling. Analysis of the catalytic currents generated by adsorbed redox enzymes requires some physicochemical modeling of the individual steps that are involved in the overall charge-transfer process, that is, substrate mass transport, reaction between enzyme and substrate, and electron exchange between enzyme and electrode. Modeling of these steps is considered next in order to obtain explicit expressions that relate the observed current to the characteristic kinetic parameters of the biosensor.

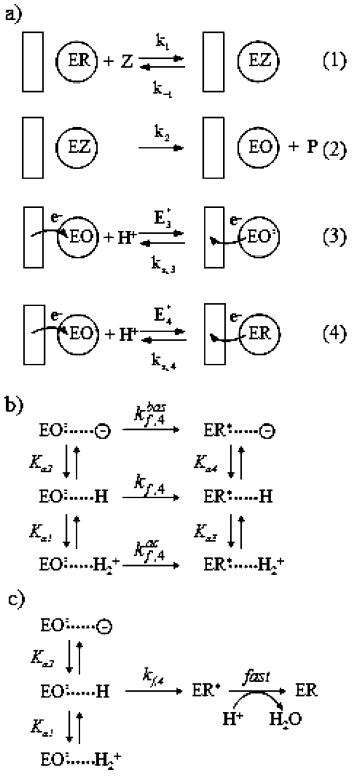

Figure 1. (a) Kinetic scheme describing the catalytic cycle of HRP under direct electron-transfer conditions, where the cosubstrate is being replaced by a graphite electrode. Abbreviations for the enzyme forms are defined in the text. (b) Square scheme for a one-electron, two-proton redox couple under irreversible electron-transfer conditions. (c) Simplified kinetic scheme accounting for the influence of solution pH on the rate of HRP Compound II reduction. Symbols are defined in the text.

The catalysis of hydrogen peroxide reduction by horseradish peroxidase has been studied extensively in the literature.[4,18] Traditionally, it has been assumed that oxidation of reduced HRP (ER) to form Compound I (EO) takes place in a single kinetic step.[4] However, experimental evidence for saturation kinetics, indicating the presence of an intermediate enzyme−substrate complex (EZ) (as depicted in Figure 1a), has been made available by using different approaches to decrease the enzymatic activity, for example, by lowering the reaction temperature,[28,29] by replacing Arginine-38 by Leucine in the catalytic pouch,[30] or by embedding HRP in a polyelectrolyte matrix.[31] Therefore, our kinetic scheme includes the formation of the Michaelis complex.

All steps in Figure 1a will be assumed to be bi-directional except for step 2, that will proceed toward the formation of Compound I only. In agreement with reported evidence in solution,[4] reduction of the adsorbed enzyme will be assumed to take place in two steps (3 and 4), each one involving the uptake of one electron from the electrode. Step 3 corresponds to the conversion of Compound I (EO) into Compound II (EO′), and step 4 corresponds to that of Compound II (EO′) into the ferric form of the enzyme (ER). Depending on the solution pH, each electron-transfer step may also involve incorporation of one proton to the protein backbone.

Moreover, it will be assumed that acquisition of kinetic data is performed in a relatively short time scale and in the presence of low enough a hydrogen peroxide concentration so that mechanistic complications associated with enzyme inhibition can be disregarded.[17]

By adopting the steady-state hypothesis, the catalytic current, i, is related to the rates of the individual steps, v_i, in a straightforward way

$$v_1 = v_2 = v_3 = v_4 = \frac{-i}{2FA} \tag{1}$$

where F stands for Faraday's constant and A stands for the electrode area. Individual rate equations can be expressed as

$$v_1 = k_1\Gamma_{ER}c_Z(0,t) - k_{-1}\Gamma_{EZ} \tag{2}$$

$$v_2 = k_2\Gamma_{EZ} \tag{3}$$

$$v_3 = k_{f,3}(\Gamma_{EO} - \Gamma_{EO'}\phi_3) \tag{4}$$

$$v_4 = k_{f,4}(\Gamma_{EO'} - \Gamma_R\phi_4) \tag{5}$$

where Γ_i is the surface concentration of the enzyme species i, $c_Z(0,t)$ is the volumetric concentration of hydrogen peroxide at the electrode surface, and

$$\phi_3 = \exp\left(\frac{F(E - E_3^*)}{RT}\right) \tag{6}$$

$$\phi_4 = \exp\left(\frac{F(E - E_4^*)}{RT}\right) \tag{7}$$

where E is the applied potential and E_3^* and E_4^* are

$$E_3^* = E^f_3 + \frac{RT}{F}\ln a_{H^+} \tag{8}$$

$$E_4^* = E^f_4 + \frac{RT}{F}\ln a_{H^+} \tag{9}$$

E_3^f and E_4^f stand for the formal potentials of steps 3 and 4, respectively. The forward charge-transfer rate constants $k_{f,3}$ and $k_{f,4}$ are exponentially related to $E - E_3^*$ and to $E - E_4^*$, respectively, through the appropriate expressions derived from either Butler−Volmer or Marcus theories.[32]

By introducing the total concentration of active enzymes

$$\Gamma_T = \Gamma_{ER} + \Gamma_{EO} + \Gamma_{EO'} + \Gamma_{EZ} \tag{10}$$

and substituting eqs 2−5 into eq 1, the following expression for the catalytic current is obtained

$$\frac{2FA}{-i} = \frac{1}{k_2\Gamma_T}\left(1 + \frac{K_M(1 + \phi_4 + \phi_3\phi_4)}{c_Z(0,t)}\right) + \frac{1}{\Gamma_T}\left(\frac{1}{k_{f,3}} + \frac{1 + \phi_3}{k_{f,4}}\right) \tag{11}$$

where $K_M = (k_{-1} + k_2)/k_1$ is Michaelis constant. The two bracketed terms on the right-hand side of eq 11 are functions of the applied potential, but only the first term varies with substrate concentration. A straightforward simplification occurs when both $E - E_3^*$ and $E - E_4^*$ are < -100 mV, then ϕ_3 and ϕ_4 become $<<1$, and eq 11 can be rewritten as:

$$\frac{2FA}{-i} = \frac{1}{k_2\Gamma_T}\left(1 + \frac{K_M}{c_Z(0,t)}\right) + \frac{1}{\Gamma_T}\left(\frac{1}{k_{f,3}} + \frac{1}{k_{f,4}}\right) \tag{12}$$

This last expression shows clearly the series connection between the electron-transfer steps and the enzyme−substrate chemical event.

Further elaboration of eq 11, or of its simplified version eq 12, is required to account for the concentration polarization of the substrate at the electrode surface. Under the steady-state conditions prevailing in rotating disk experiments, substrate concentration profiles are time-independent so that $c_Z(0,t)$ becomes simply $c_Z(0)$.

Values of $c_Z(0)$ can be derived from the observed steady-state catalytic currents as[33]

$$c_Z(0) = c_Z^* \left(1 - \frac{i}{i_L}\right) \tag{13}$$

where c_Z^* is the substrate bulk concentration and i_L is the diffusion-convection limiting current given by the Levich equation

$$\frac{-i_L}{2FA} = 0.62\nu^{-1/6} D_Z^{2/3} \omega^{1/2} c_Z^* \tag{14}$$

where D_Z, ν, and ω are the substrate diffusion coefficient, the kinematic viscosity of the solution, and the electrode rotation rate, respectively. Equation 13 can be inserted in eqs 11 and 12 to provide a simple route for the analysis of the data in the form of linear i^{-1} versus $[c_Z^*(1 - i/i_L)]^{-1}$ plots at a given potential, analogous to the classical Lineweaver−Burk plots often used in the analysis of enzyme kinetics.

B. General Characteristics of the Electrocatalytic Currents. Figure 2 illustrates the potential and substrate concentration dependence of the electrocatalytic currents measured for adsorbed HRP on a graphite electrode at three representative solution pHs, within the $4 \leq$ pH ≤ 8 range of interest. In all cases, the catalytic current becomes higher as the applied potential is made more negative and/or the hydrogen peroxide concentration is increased. However, it should also be noted that these data provide a clear indication that the influence of both parameters, potential and substrate concentration, tends to approach a saturation limit. This type of behavior is to be expected from eqs 11 and 12 because of the competing series connection between the chemical steps (the rate of which depends on concentration only, see below) and the electrochemical steps (which depend on potential but not on concentration). As shown, the catalytic current is also sensitive to the solution pH. It reaches a maximum at intermediate pH values (Figure 2b) and decreases as the solution becomes either more acidic (Figure 2a) or more basic (Figure 2c).

The kinetic analysis can be simplified by noting that the reported formal potential values of HRP Compound I (E_3^*) and Compound II (E_4^*) lie in the 0.8−1.1 V potential range;[10,11] that is, they are more than 200 mV positive with respect to the useful potential window, where significant catalytic currents can be recorded (compare E_4^* values in Table 1 with the abscissa values in Figure 2). Therefore, the ϕ_4 and $\phi_3\phi_4$ terms can be safely neglected in eq 11 and, from now on, the simplified eq 12 will be used in our kinetic analysis.

The observed catalytic currents are much smaller than the diffusion-convection limiting current i_L (typically $|i| \leq 0.2\ |i_L|$), which was computed from eq 14 by assuming $D_Z = 1.6 \times 10^{-5}$ cm^2 s^{-1}.[34] Therefore, under the present experimental conditions, concentration polarization is envisaged to play only a minor role in controlling the overall rate of the catalytic process. Though the $c_Z(0) \approx c_Z^*$ approximation is often met, no further simplifications will be pursued in our analysis. Instead, the required $c_Z(0)$ values will be computed from those of c_Z^*, i and i_L as dictated by eq 13.

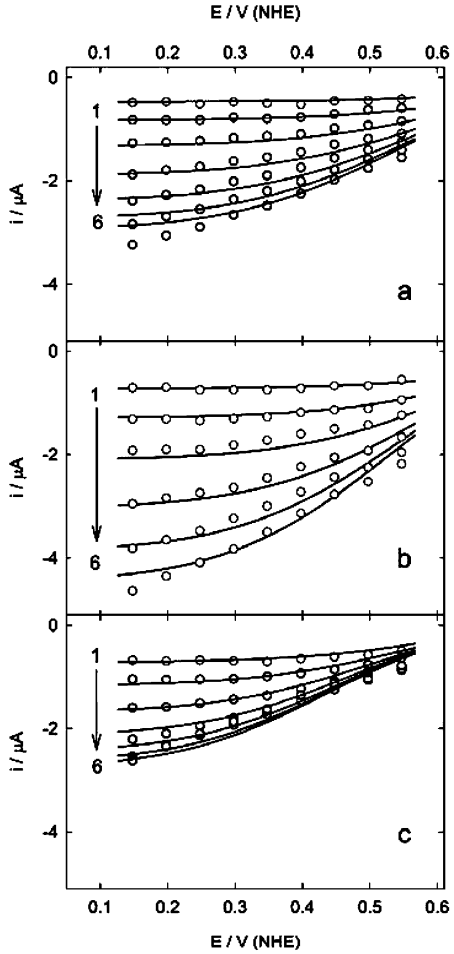

Figure 2. Steady-state catalytic currents as a function of the applied potential, hydrogen peroxide concentration, and solution pH. Open symbols are experimental values and full lines are theoretical fits, computed from eq 11 with the values of the kinetic parameters listed in Table 1. Hydrogen peroxide concentration: (1) 10 μM, (2) 20 μM, (3) 40 μM, (4) 80 μM, (5) 160 μM, (6) 320 μM. Solution pH: (a) 4.1, (b) 5.0, (c) 7.0. Electrode rotation rate is 959 rpm.

TABLE 1: Slopes of the Double Reciprocal Plots i^{-1} vs $c_Z^{-1}(0)$ (Figure 3), Total Surface Concentration of Active HRP (Γ_T), and Kinetic/Thermodynamic Parameters for the Electroreduction of HRP Compound II ($k_{s,4}$, λ_4, $k_{max,4}$ and E_4^*) at Different Solution pH Values

pH	slope ($A^{-1}M$)	$10^{13}\Gamma_T$ [a] (mol cm^{-2})	$k_{s,4}$ [a,b] (s^{-1})	λ_4 (eV)	$10^{-3}\ k_{max,4}$ [a,b] (s^{-1})	E_4^* [c] (V)
4.1	−17.7	0.9	0.7	0.60	1.6	1.073
5.0	−12.7	1.2	1.4	0.58	2.3	1.022
6.0	−13.9	1.1	3.5	0.58	5.8	0.963
7.0	−10.0	1.5	1.0	0.50	0.7	0.903
8.0	−11.0	1.4	0.9	0.43	0.3	0.841

[a] Assuming $k_2/K_M = 1.7 \times 10^7$ M^{-1} s^{-1}. [b] Assuming $k_2 = 2200$ s^{-1}. [c] From refs 10 and 11.

C. Dependence on Substrate Concentration: Decoupling of the Kinetic Terms. At a given potential, the variation of the catalytic current with substrate concentration can be exploited to disentangle the two terms appearing on the right-hand side of eq 12. Plots of i^{-1} versus $c_Z^{-1}(0)$, are found to be linear and nearly parallel in each solution (slope values are listed in Table 1), while the absolute value of the intercepts decreases monotonically as the potential is made more negative (Figure 3). Now, in this section we focus on the analysis of the slopes, whereas examination of the intercepts is postponed to the next

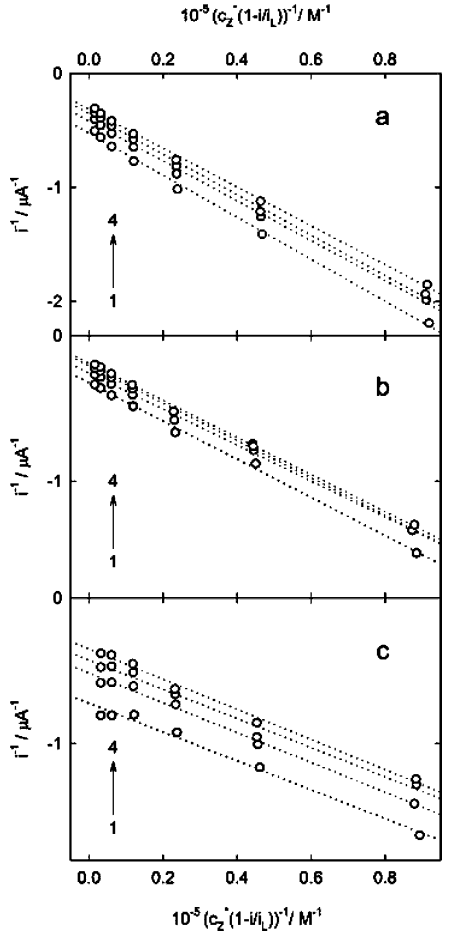

Figure 3. Double-reciprocal plot of the catalytic current against hydrogen peroxide concentration at the electrode surface, at different potential values: (1) 447 mV, (2) 347 mV, (3) 247 mV, (4) 147 mV. Open symbols are experimental values, and dotted lines are their linear least-squares fits. Solution pH: (a) 4.1, (b) 5.0, (c) 7.0. Electrode rotation rate is 959 rpm.

section where they are used to estimate the charge-transfer rate constant values.

According to eq 12, the slopes of the plots in Figure 3 are given by:

$$\left(\frac{\partial i^{-1}}{\partial c_Z^{-1}(0)}\right)_E = \frac{-K_M}{2FAk_2\Gamma_T} \tag{15}$$

so that the $k_2\Gamma_T/K_M$ ratio can be derived easily from the slope values. However, an independent estimate of the surface concentration of electrochemically active enzymes Γ_T would be required to obtain k_2/K_M. Until now, direct electrochemical determination of Γ_T for HRP has remained elusive (see ref 9 for a critical assessment of previous attempts in the literature). In fact, we could not obtain significant voltammetric currents in the absence of hydrogen peroxide, and we had to resort to an alternative approach to estimate Γ_T.

Limoges et al.[17] faced a similar problem in their analysis of the catalytic currents generated by a monolayer of HRP immobilized on a biotinylated carbon electrode. They assumed that the rate of formation of Compound I was the same in the case of adsorbed HRP molecules as that in solution. Then, by setting $k_2/K_M = 1.7 \times 10^7$ M^{-1} s^{-1}, the accepted value in solution, we can determine Γ_T from the slopes in Figure 2. In the absence of nitrate or acetate in solution, this rate constant value has been shown to be independent of the solution pH within the $4 \leq$ pH ≤ 10 range.[4] The Γ_T values listed in Table 1 were obtained by this procedure. They do not display a clear trend with the solution pH, and their differences may well be ascribed to random changes in the extent of adsorption and/or orientation from one preparative batch to another.

Because the previous procedure to determine Γ_T also affects the values of the kinetic parameters that fit our results, it may be convenient to discuss briefly its consequences. It is likely that the k_2/K_M value for the immobilized enzyme does not exceed its value for the enzyme in solution and, therefore, the tabulated values of Γ_T should be considered more strictly as lower limits of Γ_T. In fact, by comparing the analytical amount of adsorbed enzymes with the amount of electrochemically active enzymes, Limoges et al.[17] could conclude that either 75% of the immobilized enzymes remained fully active according to the "binary activity" hypothesis or, alternatively, that the overall enzymatic activity had decreased to 75% of its original value in solution upon immobilization. The crystallographic size of HRP[35] sets an upper limit of $\sim 10^{-11}$ mol cm^{-2} for a fully packed monolayer of active enzyme. However, this limit is too high to be compatible with the absence of nonturnover voltammetric currents, and a more realistic upper limit can be set at $\sim 10^{-12}$ mol cm^{-2}. Therefore, the rate constant values derived by adopting the "binary activity" hypothesis are expected to reproduce the real values within less than an order of magnitude, while reorganization energies, describing their variation with potential, are not affected by this choice.

Some additional details on the catalytic activity of HRP molecules adsorbed on graphite electrodes have been made available by comparing the catalytic current values recorded in the absence and in the presence of soluble electron-transfer mediators.[36] From this comparison, it turns out that ~50% of the active enzymes in the adsorbed layer are able to exchange electrons directly with the electrode surface. Then, the overall picture emerging from these studies is that a small number of enzymes retain their catalytic activity upon adsorbing on graphite, though a sizable number of them are involved in direct electron transfer with the electrode.

D. Dependence on Potential: The Reorganization Energy. By combining the ordinate values in Figure 3 with our previous estimates of Γ_T, we obtain at each potential the value of a first-order rate constant k_{el} (see eq 12), defined as

$$\frac{1}{k_{el}} = \frac{1}{k_2} + \frac{1}{k_{f,3}} + \frac{1}{k_{f,4}} \tag{16}$$

Within our kinetic scheme, k_{el} is simply the steady-state rate constant of a CEE charge-transfer mechanism, which includes a chemical step (C) for the formation of Compound I from the Michaelis complex (k_2) and two irreversible electron-transfer steps (EE) connected in series ($k_{f,3}$ and $k_{f,4}$). Formally, the k_2 term in eq 16 would also account for the presence of a gating process, which could limit the overall rate of charge transfer.[15,21] It is interesting that, according to eq 16, k_{el} cannot exceed the value of k_2 as the potential is made more negative (i.e., $k_{el} \leq k_2 = 2200$ s^{-1}).[18,37] Electrochemical studies allow one to vary systematically $k_{f,3}$ and $k_{f,4}$ and, possibly, to uncover the presence of a rate-limiting chemical event, such as either Compound I formation or a gating process.

Figure 4 illustrates the variation of k_{el} with potential. It can be observed how k_{el} displays a weak dependence on potential, until it levels off at sufficiently negative potential values. The slope of these plots defines an apparent charge-transfer coefficient, α, that turns out to be smaller than 0.2. This type of behavior is to be expected from the Marcus-DOS theory of

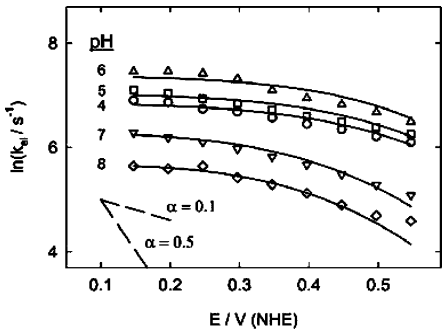

Figure 4. Dependence of the logarithm of the rate constant k_{el} on the applied potential for the indicated pHs. Full lines are theoretical fits of eq 18 to the data by assuming $k_2 = 2200\ s^{-1}$ and the Marcus-DOS expression for $k_{f,4}$ with the relevant kinetic parameters listed in Table 1. Broken lines illustrate the expected Tafel slopes for the indicated values of the charge-transfer coefficient, α.

electron transfer when the applied overpotential approaches the value of the reorganization energy (expressed in eV).[32] To reproduce the k_{el} values in Figure 4, single electron-transfer rate constants $k_{f,i}$ were expressed as[38,39]

$$k_{f,i}(\eta_i) = \frac{k_{s,i}}{Y_{f,i}} \int_{-\infty}^{\infty} \frac{\exp\left(-\dfrac{(\xi_F - \xi + e_0\eta_i + \lambda_i)^2}{4\lambda_i kT}\right)}{1 + \exp\left(\dfrac{\xi - \xi_F}{kT}\right)} d\xi \qquad (17)$$

where k is the Boltzmann constant, e_0 is the electron charge, ξ is the energy of a given electronic state in the electrode, ξ_F is the energy of the Fermi level of the electrode (i.e., e_0E where E is the applied potential), η_i is the formal overpotential of the electron-transfer step i (i.e., the applied potential relative to the formal potential E_i^*), λ_i is its reorganization energy, $k_{s,i}$ is its standard rate constant, and $Y_{f,i}$ represents the integral in eq 17 evaluated at $\eta_i = 0$.

Equation 17 can reproduce the observed potential dependence of k_{el} by just considering a single electron-transfer step, corresponding to either $k_{f,3}$ or $k_{f,4}$. Therefore, inclusion of both electron-transfer rate constants is not justified from the point of view of data fitting because it leads to kinetic overparameterization. There is broad evidence in the literature[10,23,24] showing that reduction of Compound I is 10 to 1000 times faster than reduction of Compound II in solution; therefore, it seems reasonable to assume that $k_{f,3} >> k_{f,4}$ so that eq 16 can be simplified as

$$\frac{1}{k_{el}} \approx \frac{1}{k_2} + \frac{1}{k_{f,4}} \qquad (18)$$

As illustrated in Figure 4, satisfactory fits of the k_{el} data were obtained with the $k_{s,4}$ and λ_4 values listed in Table 1 and $k_2 = 2200\ s^{-1}$. Electron-transfer standard rate constants lie in the $0.7\ s^{-1} \le k_{s,4} \le 3.5\ s^{-1}$ range, displaying a maximum at pH 6. It is interesting to compare our results with those of Heering et al.,[15] who studied the electrochemical behavior of cytochrome *c* peroxidase (C*c*P) adsorbed on graphite under both nonturnover and catalytic conditions. From their nonturnover voltammograms, they derived a surface concentration of active enzymes $\Gamma_T = 2.7 \times 10^{-12}$ mol cm^{-2}, and from the analysis of their steady-state catalytic currents they reported a value of $k_{s,4} = 7\ s^{-1}$ for the reduction C*c*P Compound II at pH = 5.8. This last result is consistent with our present estimate of $k_{s,4} \approx 3.5\ s^{-1}$ for HRP Compound II at pH = 6, and it gives further support to our previous determination of Γ_T. The low values of $k_{s,4}$ indicate that the electron exchange between graphite and Compound II is considerably less efficient than that between the archetypical redox protein cytochrome *c* and gold or silver, for which k_s values higher than $100\ s^{-1}$ have been reported.[21,40,41] The combination of a weaker electronic coupling, associated with the bigger molecular size of peroxidases, together with a lower density of electronic states of graphite[42] helps to rationalize such differences in reactivity.

As shown in Table 1, reorganization energies remain close to 0.6 eV up to pH 6, and then decrease to 0.4 eV as the solution pH increases to 8. To our knowledge, this is the first time that the reorganization energy for Compound II reduction has been reported. In a similar analysis of C*c*P Compound II reduction,[15] the value of the reorganization energy remained elusive because of the kinetic interference of a slow chemical step with $k_{chem} \approx 300\ s^{-1}$. Such a slow chemical step is likely to be absent in the case of HRP, where physically reasonable reorganization energies are obtained and k_{el} values as high as $1700\ s^{-1}$ have been recorded (Figure 4).

Miller et al.[43] have obtained values of 0.58 and 0.43 eV for the reorganization energies of cytochromes *c* and b_5, respectively. They also derived a value of 0.41 eV for the inner sphere reorganization energy of bis(*N*-methylimidazole)-*meso*-tetraphenyl iron porphyrin, which can be considered as a simplified chemical model of the redox active center in heme proteins. From the similarity between this last value and the reorganization energies of the two cytochromes, they concluded that the protein matrix mimics the behavior of a low dielectric solvent and effectively shields the heme from the solvent. The further coincidence of their results with our own values in Table 1 suggests that the stretching frequencies associated with the porphyrin ring provide the main contribution to the reorganization energy values of Compound II.

We have also considered the possibility that the weak dependence of the catalytic current on potential could arise from a distribution of electron-transfer tunneling distances, as described by Léger et al.,[44] rather than from the saturation of the electron-transfer rate values when the thermodynamic driving energy becomes comparable to the reorganization energy. However, no satisfactory fits of our results could be obtained with the expression for the catalytic current derived from the Léger et al. model.

E. Dependence on Solution pH: Search of the Electron Pathway. As stated above, the catalytic activity of HRP adsorbed on graphite electrodes varies parabolically with the solution pH, reaching a maximum at a pH close to 6. Because the rate of formation of Compound I is independent of the solution pH for $9 \ge$ pH ≥ 4,[4] it seems reasonable to ascribe the observed pH dependence to the reduction of Compound II in the reaction scheme depicted in Figure 1a. Figure 5a illustrates how $-\ln(k_{el}^{-1} - k_2^{-1})$ ($\equiv \ln k_{f,4}$) reproduces, at a given potential, the overall pH dependence of the catalytic activity. It should be noted that k_{el} and k_2 take similar values at $E \approx 0.2$ V and pH ≈ 6, thereby rendering the determination of $k_{f,4}$ rather inaccurate under these circumstances. Within the framework of the non-adiabatic Marcus theory, the rate of electron transfer is controlled by the reorganization energy, the thermodynamic driving force, and the donor/acceptor electronic coupling. Neither of the first two factors can explain the observed pH dependence of k_{el}; let us consider now the behavior of the electronic coupling term.

At high enough overpotentials, the Marcus-DOS electron-transfer rate constants described by eq 17 reach a potential

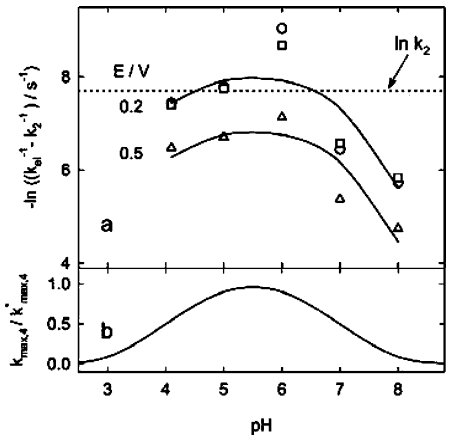

Figure 5. (a) Dependence of the logarithm of the $k_{el}^{-1} - k_2^{-1}$ ($\equiv k_{f,4}$) difference on the solution pH, at a given $E = 0.2$ V (○), 0.5 V (Δ), and at the $E \rightarrow -\infty$ limit (□), that defines $k_{max,4}$ according to eq 19 in the text. The dotted line is an eyeguide to locate the value of ln k_2 in the plot. Full lines are theoretical fits of eq 20 to the data. (b) Variation of the electronic coupling efficiency with solution pH according to eq 20.

independent plateau, which defines

$$k_{max,4} = k_{f,4}\,(\eta_4 \rightarrow -\infty) \qquad (19)$$

the value of which is determined in the non-adiabatic limit by the electronic coupling between the electrode and the enzymatic redox center and by the density of electronic states at the electrode.[15,38,45,46] Values of $k_{max,4}$ are depicted in Figure 5 (and collected also in Table 1) as a function of pH, and they are seen to be very close to those of $k_{f,4}$ obtained at $E = 0.2$ V. Their dependence on solution pH, dictated by changes in the electronic coupling, contrasts with the linear variation of the equilibrium formal potential E_4^* with pH (see Table 1), whose slope value of 60 mV/decade[10,11] indicates that reduction of Compound II is accompanied by a proton uptake. At least two pK_a values are required to account for the parabolic dependence of the reduction rate of Compound II on solution pH. According to the 1 e^--2 H^+ scheme depicted in Figure 1b under irreversible electron-transfer conditions, $k_{max,4}$ can be expressed as[47]

$$k_{max,4} = \frac{k_{max,4}^{ac}\,(c_{H^+}/K_{a1}) + k_{max,4}^{*} + k_{max,4}^{bas}\,(K_{a2}/c_{H^+})}{(c_{H^+}/K_{a1} + 1 + K_{a2}/c_{H^+})} \qquad (20)$$

where $k_{max,4}^{ac}$, $k_{max,4}^{*}$ and $k_{max,4}^{bas}$ are the maximum electron-transfer rate constants for the acid, neutral, and basic reaction pathways, respectively, and K_{a1} and K_{a2} are the equilibrium constants for the two protonation equilibria controlling the observed pH dependence. Note that K_{a3} and K_{a4} do not appear in eq 20 because the irreversible nature of the electron-transfer steps at such high overvoltage values. The three terms in brackets in eq 20 determine the relative amounts of each protonated form at a given pH. To obtain a maximum in the pH dependence of $k_{max,4}$, it is required that $k_{max,4}^{*} > k_{max,4}^{ac}$, $k_{max,4}^{bas}$. However, a quantitative determination of $k_{max,4}^{ac}$ and $k_{max,4}^{bas}$ is prevented by the limited accuracy of our data and the restricted pH range available. Therefore, we have further simplified our previous kinetic scheme as depicted in Figure 1c.

Figure 1c shows the simplest kinetic scheme accounting simultaneously for the observed variations of E_4^* and $k_{max,4}$ with pH. This scheme implies that electron tunneling from the electrode is restricted to a particular protonation state of the enzyme (EO′--H in Figure 1c), and that a fast proton transfer follows the rate-determining electron-transfer step. The reverse process has been studied by Gray et al.,[48] who showed that photoinduced oxidation of the resting enzyme involves a fast generation of a π-cation porphyrin radical, which is followed by a slow binding of a water molecule to form Compound II. In a similar way, the kinetic scheme in Figure 1c would be consistent with an initial electron uptake, to be followed by the removal of the oxo atom as part of the leaving water molecule.

According to Figure 1c, the pH dependence of $k_{max,4}$ can be described by[47]

$$k_{max,4} = \frac{k_{max,4}^{*}}{(c_{H^+}/K_{a1} + 1 + K_{a2}/c_{H^+})} \qquad (21)$$

This expression defines the pK_{a2} > pH > pK_{a1} interval, where efficient electron exchange between enzyme and electrode takes place through the EO′--H electroactive form of the enzyme. The maximum electron-transfer rate constant for this useful reaction path is $k_{max,4}^{*}$. A reasonable fit of the $k_{max,4}$ values is obtained with p$K_{a1} = 4$, p$K_{a2} = 7$, and $k_{max,4}^{*} = 3 \times 10^3$ s^{-1} (Figure 5).

The rate of oxidation of several phenols by HRP Compound II in solution reaches a broad maximum at pH ≈ 7, and its pH dependence seems to be controlled by two protonation equilibria with p$K_{a1} \approx 4.5$ and p$K_{a2} \approx 8.5$.[26,27] The first value has been ascribed to a heme linked propionic group, and the second to the distal histidine His-42, hydrogen bonded to the oxyferryl group. Similar assignments are difficult to make in the case of these electrochemical experiments because of the lack of information on the orientation of the electroactive enzymes at the electrode surface and, therefore, on the location of the electronic path. Still, some information on the involvement of amino acid residues in the reduction of Compound II can be reached by comparing the variations of the reorganization energy and the electronic coupling with pH.

Upon varying the solution pH from 4 to 6, the electronic coupling between enzyme and electrode increases, whereas the reorganization energy remains unchanged. Therefore, the p$K_{a1} = 4$ ionization equilibrium should be ascribed to a carboxylic group located in (or nearby) the electronic path, but sufficiently far from the porphyrin ring so that its protonation state does not influence the reorganization energy. The apparent increase in electronic conductivity upon ionization of a carboxylic group is supported by recent theoretical and experimental studies on the rate of electron transfer through functionalized thiol monolayers that expose either carboxylic or phenolic end groups to the solution.[49,50] Heme propionates are obvious candidates for the assignment of pK_{a1}, but other alternatives, including carboxylic groups generated by oxidation of the carbon electrode surface, cannot be excluded.

A further increase in the solution pH from 6 to 8 causes a decrease of both the electron-transfer reorganization energy and the electronic coupling. The simultaneity of these two effects is consistent with an increase of the π charge delocalized over the porphyrin ring, as a consequence of the pK_{a2} ionization process. By increasing the electronic charge density, the oxidized heme group would approach the structure of the electron-transfer product, thereby reducing the energetic cost for electron-transfer reorganization. At the same time, the increase of negative charge on the ring diminishes the probability of electron transfer from the electrode.[51] This type of π-electron injection coupled to an acid/base equilibrium has been shown to occur in the case of ferrous HRP, as a consequence of the distal histidine depro-

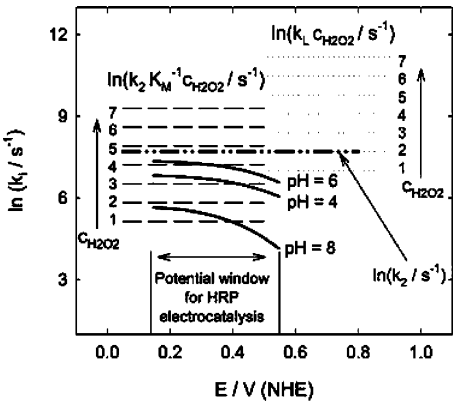

Figure 6. Comparison of the kinetic terms contributing to the observed catalytic currents. Solid lines: ln k_{el} as a function of potential at the indicated pH values. Dashed lines: logarithm of the apparent Michaelis rate constant $k_2 K_M^{-1}$ for low substrate concentration at the indicated substrate concentrations. Dotted lines: logarithm of the apparent mass transport rate constant $k_L c_{H_2O_2} = i_L/nFA\Gamma_T$, at the indicated substrate concentrations. Dotted and dashed line: logarithm of the catalytic rate constant k_2. Substrate concentrations: (1) 10 μM, (2) 20 μM, (3) 40 μM, (4) 80 μM, (5) 160 μM, (6) 320 μM, (7) 640 μM.

tonation.[52] Dunford[53] has proposed that a highly conserved network of hydrogen bonds, which links the distal and proximal histidine residues, might provide the electronic path connecting the distal histidine to the porphyrin ring. This heme linked ionization equilibrium exhibits a value of pK_a = 7.1 for the ferrous enzyme,[52] but it raises to 8.5 for HRP Compound II.[54] The difference of ~1.5 units between the distal histidine pK_a in Compound II and the observed pK_{a2} value hinders a straightforward assignment of this last value. In any case, the strong influence of the ionization process on the reorganization energy indicates that it should be ascribed to an amino acid residue located around the heme pocket.

Concluding Remarks

Electrocatalytic currents generated by adsorbed enzymes with a single active site are determined by the rates of three processes, namely, substrate mass transport, substrate reaction at the active site, and electron exchange between the active site and the electrode. The use of the rotating disk electrode helps to enhance the rate of mass transport and to set steady-state conditions, where the kinetics of the last two processes can conveniently be studied. The kinetic contributions of these three processes to the observed catalytic currents are compared in Figure 6. It may be observed that as the hydrogen peroxide concentration increases, the kinetic control shifts from catalytic turnover to electron transfer to HRP Compound II, but substrate mass transport never becomes rate-determining. The distinct dependence of the substrate/enzyme reaction and the electrode/enzyme electron exchange on substrate concentration and electrode potential allows us to disentangle their individual contributions to the observed current. In the case of adsorbed HRP, this simple analysis benefits from the wealth of information, which is available on HRP catalysis, but it is hampered by the absence of observable nonturnover currents that prevents a direct determination of the number of active enzymes. This difficulty has been circumvented by adopting the "binary activity" hypothesis,[15,17] which leads to consistent results and suggests that the absence of nonturnover signals is due to the small number of active enzymes. Upon studying the rates of electron transfer to, or from, an active site of an enzyme, the electrochemical techniques can provide a straightforward route to the determination of the reorganization energy. The low value of the reorganization energy found for HRP Compound II reduction (~0.5 eV) seems to support the role of the low dielectric permittivity of the medium that surrounds the active site as a key contribution to the catalytic efficiency of enzymes. The distinct variations of the reorganization energy and of the electrode/enzyme electronic coupling with solution pH offer some useful hints on the nature and location of the acid/base groups that interact with the electron-transfer pathway.

Acknowledgment. J.J.C. and R.A. acknowledge financial support from the DGICYT under grant CTQ 2005-01184, E.E.F. thanks the Wenner-Gren Foundation for funding. and L.G. acknowledges the financial support from The Swedish Research Council.

References and Notes

(1) (a) Ferapontova, E. E.; Shleev, S.; Ruzgas, T.; Stoica, L.; Christenson, A.; Tkac, J.; Gorton, L. In *Electrochemistry of Nucleic Acids and Proteins*; Palacek, E., Scheller, F. W., Wang, J., Eds.; Elsevier: Amsterdam, 2005; Vol. 1, pp 517−598. (b) Wollenberger, U. In *Comprehensive Analytical Chemistry*; Gorton, L., Ed.; Elsevier: Amsterdam, 2005; Vol. XLIV, pp 65−130.

(2) Ghindilis, A. L.; Atanasov, P.; Wilkins, E. *Electroanalysis* **1997**, *9*, 661.

(3) Léger, C.; Elliot, S. J.; Hoke, K. R.; Jeuken, L. J. C.; Jones, A. K.; Armstrong, F. A. *Biochemistry* **2003**, *29*, 8653.

(4) Dunford, H. B. *Heme Peroxidases*; Wiley: New York, 1999.

(5) (a) Ryan, O.; Smyth, M. R.; O'Fagain, C. In *Essays in Biochemistry*; Ballou, D. K., Ed.; Portland Press: London, 1994; Vol. 28, pp 129−146. (b) Ruzgas, T.; Csöregi, E.; Emnéus, J.; Gorton, L.; Marko-Varga, G. *Anal. Chim. Acta* **1996**, *330*, 123. (c) Narváez, A.; Suarez, G.; Popescu, I. C.; Katakis, I.; Domínguez, E. *Biosens. Bioelectron.* **2000**, *15*, 43.

(6) Berglund, G. L.; Carlsson, G. H.; Smith, A. T.; Szöke, H.; Henriksen, A.; Hadju, J. *Nature* **2002**, *417*, 463.

(7) Yaropolov, A. I.; Tarasevich, M. R.; Varfolomeev, S. D. *Bioelectrochem. Bioenerg.* **1978**, *5*, 18.

(8) Ferapontova, E. E. *Electroanalysis* **2004**, *16*, 1101.

(9) Ruzgas, T.; Lindgren, A.; Gorton, L.; Hecht, H.; Reichelt, J.; Bilitewski, U. In *Electroanalytical Methods for Biological Materials*; Brajter-Toth, A., Chambers, J. Q., Eds.; Marcel Dekker: New York, 2002; pp 233−254.

(10) Hayashi, Y.; Yamazaki, I. *J. Biol. Chem.* **1979**, *254*, 9101.

(11) He, B.; Sinclair, R.; Copeland, B. R.; Makino, R.; Powers, L. S.; Yamazaki, I. *Biochemistry* **1996**, *35*, 2413.

(12) Shleev, S.; Jarosz-Wilkolazka, A.; Khalunina, A.; Morozova, O.; Yaropolov, A.; Ruzgas, T.; Gorton, L. *Bioelectrochem.* **2005**, *67*, 115.

(13) Rüdiger, O.; Abad, J. M.; Hatchikian, E. C.; Fernandez, V. M.; De Lacey, A. L. *J. Am. Chem. Soc.* **2005**, *127*, 16008.

(14) Sethuraman, A.; Belfort, G. *Biophys. J.* **2005**, *88*, 1322.

(15) Heering, H. A.; Hirst, J.; Armstrong, F. A. *J. Phys. Chem. B* **1998**, *102*, 6889.

(16) Lyons, M. E. G. *Sensors* **2002**, *2*, 473.

(17) Limoges, B.; Savéant, J. M.; Yazidi, D. *J. Am. Chem. Soc.* **2003**, *125*, 9192.

(18) Dequaire, M.; Limoges, B.; Moiroux, J.; Savéant, J. M. *J. Am. Chem. Soc.* **2002**, *124*, 240.

(19) Marcus, R. A.; Sutin, N. *Biochim. Biophys. Acta.* **1985**, *811*, 265.

(20) Moser, C. C.; Dutton, P. L. In *Protein Electron Transfer*; Bendall, D. S. Ed.; Bios Scientific Publishers: Oxford, 1996; pp 1−21.

(21) Jeuken, L. J. C. *Biochim. Biophys. Acta.* **2003**, *1604*, 67.

(22) Gajhede, M. In *Handbook of Metalloproteins*; Messerschmidt, A., Ed.; John Wiley & Sons: Chichester, 2001; pp 195−210.

(23) Folkes, L. K.; Candeias, L. P. *FEBS Lett.* **1997**, *412*, 305.

(24) Khopde, S. M.; Priyadarsini, K. I. *Biophys. Chem.* **2000**, *88*, 103.

(25) Ferapontova, E. E.; Gorton, L. *Bioelectrochem.* **2002**, *55*, 87.

(26) Critchlow, J. E.; Dunford, H. B. *J. Biol. Chem.* **1972**, *247*, 3714.

(27) Patel, P. K.; Mondal, M. S.; Modi. S.; Behere, D. V. *Biochim. Biophys. Acta.* **1997**, *1339*, 79.

(28) Baek, H. K.; Van Wart, H. E. *Biochemistry* **1989**, *28*, 5714.

(29) Baek, H. K.; Van Wart, H. E. *J. Am. Chem. Soc.* **1992**, *114*, 718.

(30) Rodríguez-López, J. N.; Smith, A. T.; Thorneley, R. N. F. *J. Biol. Chem.* **1996**, *271*, 4023.

(31) Calvente, J. J.; Narváez, A.; Domínguez, E.; Andreu, R. *J. Phys. Chem. B* **2003**, *107*, 6629.

(32) Schmickler, W. *Interfacial Electrochemistry*; Oxford University Press: New York, 1996.

(33) Bard, A. J.; Faulkner, L. R. *Electrochemical Methods*; Wiley: New York, 2001.
(34) Prabhu, V. G.; Zarapkar, L. R.; Dhaneshwar, R. G. *Electrochim. Acta.* **1981**, *26*, 725.
(35) Henriksen, A.; Smith, A. T.; Gajhede, M. *J. Biol. Chem.* **1999**, *274*, 35005.
(36) (a) Ruzgas, T.; Gorton, L.; Emnéus, J.; Marko-Varga, G. *J. Electroanal. Chem.* **1995**, *391*, 41. (b) Lindgren, A.; Munteanu, F. D.; Gazaryan, I. G.; Ruzgas, T.; Gorton, L. *J. Electroanal. Chem.* **1998**, *458*, 113.
(37) Rodríguez-López, J. N.; Gilabert, M. A.; Tudela, J.; Thorneley, R. N. F.; García-Cánovas, F. *Biochemistry* **2000**, *39*, 13201.
(38) Chidsey, C. E. D. *Science* **1991**, *251*, 919.
(39) Weber, K.; Creager, S. E. *Anal. Chem.* **1994**, *66*, 3164.
(40) Murgida, D. H.; Hildebrandt, P. *J. Am. Chem. Soc.* **2001**, *123*, 4062.
(41) Khostariya, D. E.; Wei, J.; Liu, H.; Yue, H.; Waldeck, D. H. *J. Am. Chem. Soc.* **2003**, *125*, 7704.
(42) Gerischer, H.; McIntyre, R.; Scherson, D.; Storck, W. *J. Phys. Chem.* **1987**, *91*, 1930.
(43) Blankman, J. I.; Shahzad, N.; Dangi, B.; Miller, C. J.; Guiles, R. D. *Biochemistry* **2000**, *39*, 14799.
(44) Léger, C.; Jones, A. K.; Albracht, P. J.; Armstrong, F. A. J. *J. Phys. Chem. B* **2002**, *106*, 13058.
(45) Becka, A. M.; Miller, C. J. *J. Phys. Chem.* **1992**, *96*, 2657.
(46) Finklea, H. O.; Yoon, K.; Chamberlain, E.; Allen, J.; Haddox, R. *J. Phys. Chem. B* **2001**, *105*, 3088.
(47) Finklea, H. O. *J. Phys. Chem. B* **2001**, *105*, 8685.
(48) Berglund, J.; Pascher, T.; Winkler, J. R.; Gray, H. B. *J. Am. Chem. Soc.* **1997**, *119*, 2464.
(49) Calvente, J. J.; López-Pérez, G.; Ramírez, P.; Fernández, H.; Zón, M. A.; Mulder, W. H.; Andreu, R. *J. Am. Chem. Soc.* **2005**, *127*, 6476.
(50) Ramírez, P.; Andreu, R.; Calvente, J. J.; Calzado, C. J.; López-Pérez, G. *J. Electroanal. Chem.* **2005**, *582*, 179.
(51) Calzado, C. J.; Malrieu, J.-P.; Sanz, J. F. *J. Phys. Chem. A* **1998**, *102*, 3659.
(52) Shelnutt, J. A.; Alden, R. G.; Ondrias, M. R. *J. Biol. Chem.* **1986**, *261*, 1720.
(53) Dunford, H. B. *J. Biol. Inorg. Chem.* **2001**, *6*, 819.
(54) Sitter, A. J.; Reczek, C. M.; Terner, J. *J. Biol. Chem.* **1985**, *260*, 7515.